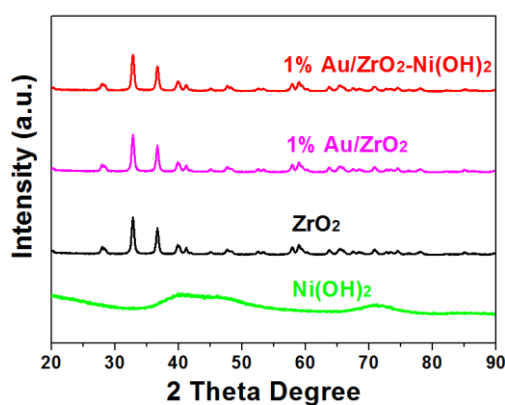


Plasmon Enhanced Nickel(II) Catalyst for Photocatalytic Lignin Model Cleavage

Yichao Jin ^{1,†}, Xiayan Wu ^{1,†}, Sarina Sarina ¹, Yingping Huang ^{2,*}, Eric R. Waclawik ¹, and Huaiyong Zhu ^{1,*}Table S1. ICP-OES test for 1 wt% Au/ZrO₂-Ni(OH)₂.

Element	Percentage
Au	1.05 % (Catalytic design is 1 wt% Au)
Ni	1.41 % (Calculated theoretical 0.02 mmol Ni =1.56 %)

Figure S1. XRD for 1% Au/ZrO₂ and Au/ZrO₂-Ni(OH)₂ catalyst.

XRD patterns indicate that Au NPs and Ni(OH)₂ have a negligible impact on the ZrO₂ crystal structure due to the low amount of loading. It clearly shows that all diffraction peaks could be indexed to a monoclinic structure of ZrO₂ crystal (JCPDS, No. 65-2357). The XRD patterns showed no trace of Au, probably because the NP size is too small and evenly distributed. Ni(OH)₂ has been independently synthesized with identical conditions except for the Au/ZrO₂ involved. XRD showed it has an amorphous structure.

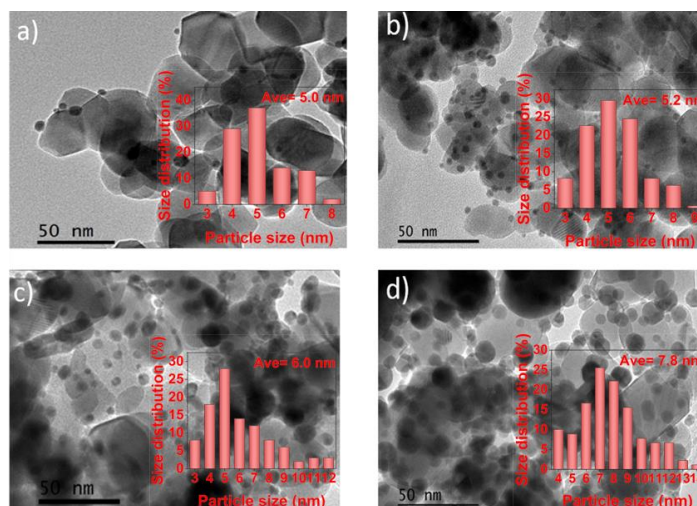


Figure S2. TEM images of the Au/ZrO₂ catalysts with different Au loading (a) Au/ZrO₂ (0.5 wt%), (b) Au/ZrO₂ (3.0 wt%), (c) Au/ZrO₂ (5.0 wt%) and (d) Au/ZrO₂ (10.0 wt%).

Figure S2 showed that with increased Au loading, Au particle size gradually increased, e.g., 1 wt% Au/ZrO₂ has a particle size of 5.0 nm, and 10 wt% Au/ZrO₂ has a particle size of 7.8 nm.

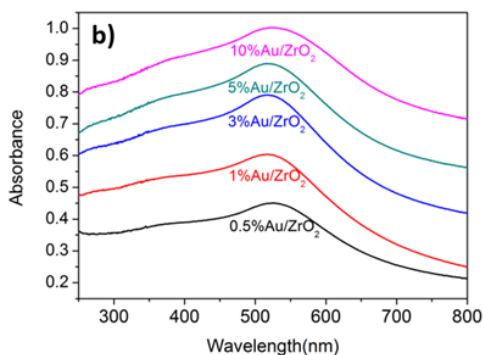


Figure S3. UV-Vis spectra of Au/ZrO₂ with different amounts of Au loading.

UV-Vis spectra (Figure S3) showed that higher Au loading leads to stronger light absorption.

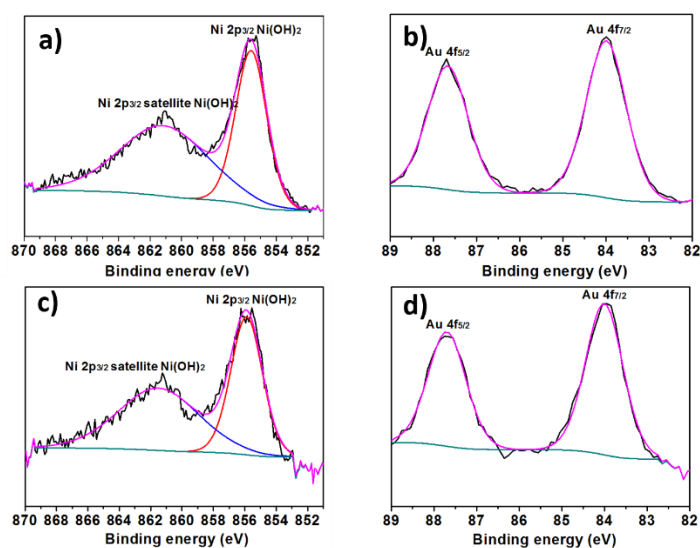


Figure S4. Au and Ni XPS of the 1wt% Au/ZrO₂-Ni(OH)₂ catalyst a) and b) before and c) and d) after the reaction.

XPS showed that the binding energy (BE) of Ni 2p_{3/2} of the 1%Au/ZrO₂-Ni(OH)₂ catalyst before the reaction has two distinct peaks at 855.6 eV and 861.1eV which indicates Ni(OH)₂ species and its satellite peak (Fig. S4a)^[1]. The BE of Au 4f_{7/2} and Au 4f_{5/2} electrons are 84.0 eV and 87.7 eV, respectively (Fig. S4b), which suggests that Au exists in the metallic state^[2]. The XPS analysis of the catalyst after the reaction suggests that the chemical condition of Ni and Au is maintained the same as before the reaction (Fig. S4c and S4d).

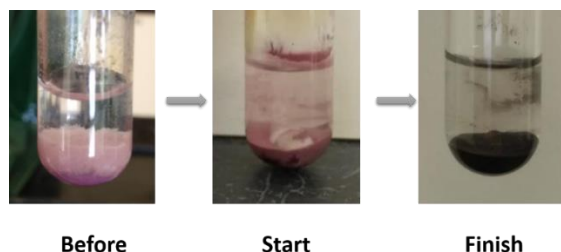


Figure S5. Left: before the reaction, Ni(OH)₂ formed on top of Au/ZrO₂. Middle: Start reaction can mix Ni(OH)₂ and Au/ZrO₂ well. Right: After the reaction catalyst colour changes due to the reduction of Ni(OH)₂ to Ni⁰.

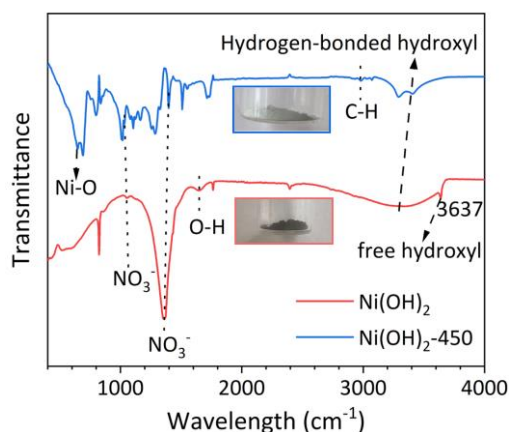


Figure S6. FTIR spectra of fresh Ni(OH)₂ and after calcination at 450 °C for 1 h in the air (labeled as Ni(OH)₂-450). The Ni(OH)₂ is synthesized using the same ratio of Ni(NO₃)₂ with KOH in IPA as used to prepare Au/ZrO₂-Ni(OH)₂ catalyst. The photographs of samples are inserted under their spectra.

We confirmed the formation of NiO with the FTIR spectra in Fig. S6. Due to the strong stretching vibration bond of Zr-O and Zr-O-Zr at 600-800 cm⁻¹, overlapping the Ni-O stretching vibration mode, we cannot observe any transformation information by FTIR using Au- Ni(OH)₂ and Au/ZrO₂-450 °C-NiO. Besides, the dehydration of Ni(OH)₂ was also confirmed by FTIR in Fig. S6. The sharp band at 3637 cm⁻¹ is a characteristic peak of β-Ni(OH)₂, owing to the stretching vibration mode of the free hydroxyl group^[3,4]. After the calcination process, this peak disappeared, indicating that Ni(OH)₂ is decomposed. The peak at 647 cm⁻¹ is attributed to the Ni-O stretching vibration mode^[5].

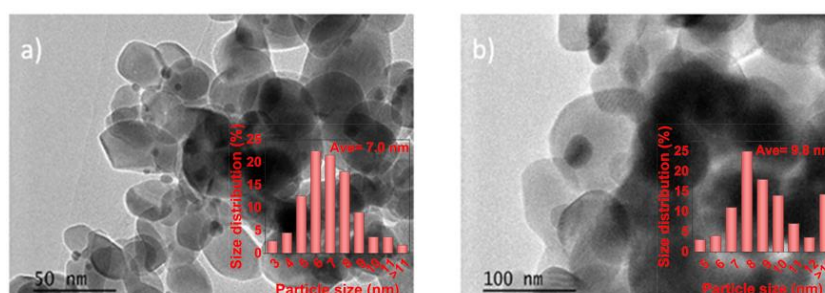


Figure S7. TEM images of a) Calcine 1 % Au/ZrO₂ at 450 °C for 1 h. b) Calcine 1 % Au/ZrO₂ at 600 °C for 4 h.

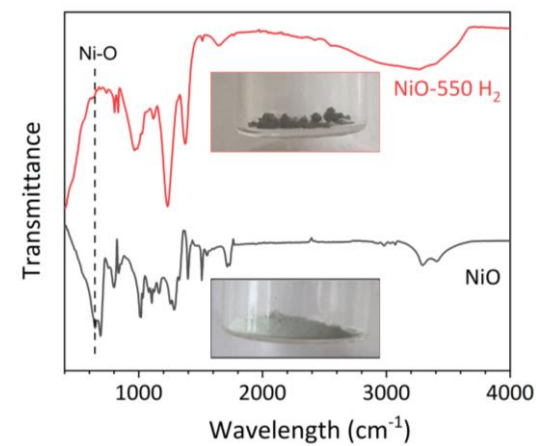


Figure S8. FTIR spectra of NiO formed calcination of Ni(OH)₂ at 450 °C for 1 h in the air (black line) and after reduction of this NiO sample at 550 °C for 0.5 h in the H₂ atmosphere (labeled as NiO-550 H₂, red line). The photographs of samples are inserted under their spectra.

After the reduction process, no stretching vibration mode of the free hydroxyl group is observed. The sharp peak at 646 cm⁻¹ (Ni-O stretching vibration mode) diminished significantly, indicating the part of NiO has been reduced to Ni⁰ sites.

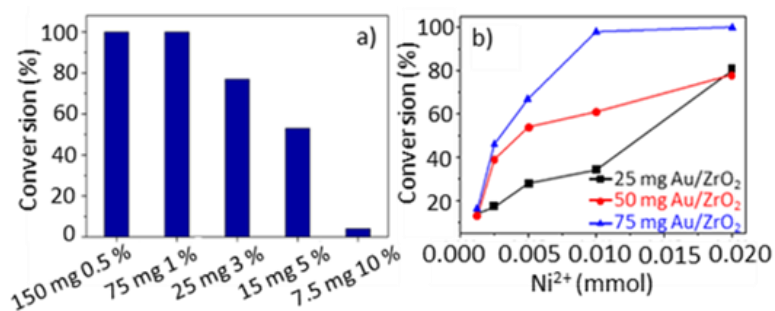


Figure S9. a) Photocatalytic reaction α -O-4 lignin model cleavage with Au/ZrO₂ catalyst with different Au loading. b) Photocatalytic reaction α -O-4 lignin model cleavage with different amounts of 1 wt% Au/ZrO₂ catalyst and different amounts of Ni²⁺.

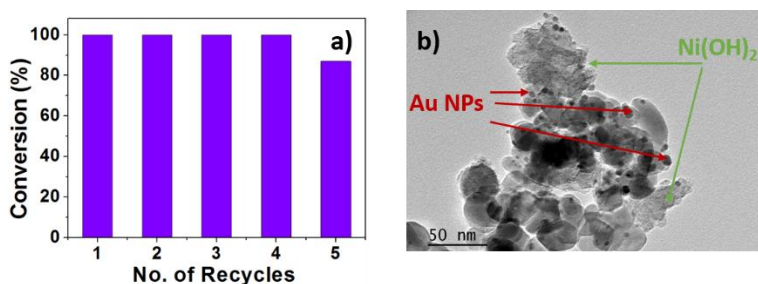


Figure S10. a) The reusability of the Au/ZrO₂-Ni(OH)₂ catalyst for α -O-4 cleavage under the base-free reaction condition. b) TEM of Au/ZrO₂-Ni(OH)₂ catalyst after the fifth cycle.

In the experiments, an excessive base is used to precipitate nickel hydroxide in the reaction (The theoretical amount of Ni²⁺: OH ratio is 1:2 in Ni(OH)₂, but 5 times KOH is added to precipitate Ni²⁺). To investigate the synergistic effect of Au NPs with Ni(OH)₂ without the excessive base, the catalyst from the first run was washed with IPA three times, dried in the vacuum oven and reused but without adding further KOH. To our surprise, Au/ZrO₂-Ni(OH)₂ exhibits good reusability, as shown in Fig. S10a. The reaction conversion maintained 100 % for four cycles and slightly decreased at the fifth cycle while selectivity was still towards a 1:1 ratio between toluene and phenol under the base-free condition. These results also suggest that the Au/ZrO₂ and Ni(OH)₂ are strongly bonded, and the leaching of the Au/ZrO₂ and Ni(OH)₂ from the photocatalyst during the photocatalytic reactions is negligible. It means the hydroxyl component in

the Ni(OH)₂ acts as the base to drive the reaction. TEM (Fig S10b) shows that after five times recycling, the catalyst keeps the morphology before the reaction. If we add new Ni(NO₃)₂/IPA solution and KOH in the recycle run, the reaction cannot even start. This indicates that newly formed Ni(OH)₂ hinders the catalytic activity of Au/ZrO₂-Ni(OH)₂, and the advantage of the LSPR effect from Au NPs has been blocked. It may be because the Ni(OH)₂ in Au/ZrO₂-Ni(OH)₂ is partially reduced to Ni⁰. If the newly formed Ni(OH)₂ is added and covers Ni⁰, the reactant cannot contact Ni⁰. Thus, the reaction cannot start.

Reference

1. Biesinger, M.C.; Lau, L.W.; Gerson, A.R.; Smart, R.S.C. The role of the Auger parameter in XPS studies of nickel metal, halides and oxides. *Phys. Chem. Chem. Phys.* **2012**, *14*, 2434–2442.
2. Casaletto, M.P.; Longo, A.; Martorana, A.; Prestianni, A.; Venezia, A.M. *Surf. Interface Anal.* **2006**, *38*, 215–218.
3. Kaspar, J.; Bazarjani, M.S.; Schitco, C.; Gurlo, A.; Graczyk-Zajac, M.; Riedel, R. Electrochemical study of NiO nanosheets: Toward the understanding of capacity fading. *J. Mater. Sci.* **2017**, *52*, 6498–6505.
4. Zhang, S.; Zeng, H.C. Self-Assembled Hollow Spheres of β-Ni(OH)₂ and Their Derived Nanomaterials. *Chem. Mater.* **2009**, *21*, 871–883.
5. Wei, Z.; Qiao, H.; Yang, H.; Zhang, C.; Yang, X. Characterization of NiO nanoparticles by anodic arc plasma method. *J. Alloys Compd.* **2009**, *479*, 855–858.